International Journal of Mass Spectrometry 303 (2011) 15–26

Contents lists available at ScienceDirect

International Journal of Mass Spectrometry

journal homepage: www.elsevier.com/locate/ijms

# Real-time aerosol mass spectrometry with millisecond resolution

Joel R. Kimmel[a,b,c], Delphine K. Farmer[c,d], Michael J. Cubison[c,d], Donna Sueper[a,c], Christian Tanner[b], Eiko Nemitz[e], Douglas R. Worsnop[a], Marc Gonin[b], Jose L. Jimenez[c,d,*]

[a] Aerodyne Research Inc., Billerica, MA, USA
[b] Tofwerk AG, Thun, Switzerland
[c] Cooperative Institute for Research in Environmental Sciences, University of Colorado, Boulder, CO, USA
[d] Department of Chemistry and Biochemistry, University of Colorado, Boulder, CO, USA
[e] Atmospheric Sciences, Centre for Ecology and Hydrology (CEH), Edinburgh, Bush Estate, Penicuik, Midlothian, UK

ARTICLE INFO

*Article history:*
Received 16 August 2010
Received in revised form 7 December 2010
Accepted 7 December 2010
Available online 23 December 2010

*Keywords:*
Aerosol
Time-of-flight
Mass spectrometry
Analog-to-digital converter (ADC)
Eddy covariance flux

ABSTRACT

The time-of-flight aerosol mass spectrometer (ToF-AMS) determines particle size by measuring velocity after expansion into vacuum and analyzes chemical composition by thermal vaporization and electron ionization mass spectrometry (MS). Monitoring certain dynamic processes requires the ability to track changes in aerosol chemistry and size with sub-second time resolution. We demonstrate a new ToF-AMS data acquisition mode capable of collecting high-resolution aerosol mass spectra at rates exceeding 1 kHz. Coupled aerosol size and MS measurements can be made at approximately 20 Hz. These rates are about 1/10 of the physically meaningful limits imposed by the ToF-AMS detection processes. The fundamentals of the time-of-flight MS (TOFMS) data acquisition system are described and characterized with a simple algebraic model. Derived expressions show how improvements in data acquisition and computer hardware will translate into rates approaching the physical limits. Conclusions regarding limits of performance can be extended to other TOFMS that use analog signal detection in a high-speed application outside of aerosol science. The high-speed acquisition mode of the ToF-AMS enables speciated aerosol eddy covariance flux measurements, which demand precise, 10-Hz synchronization of the MS with a sonic anemometer. Flux data acquired over a forest during the BEARPEX-1 campaign are presented as an example of this new technique. For aircraft measurements, faster acquisition translates to higher spatial resolution, which is demonstrated with data from the recent NASA ARCTAS field campaign in Alaska. Finally, the fast acquisition mode is used to measure the rapid fluctuations in particle emissions of a controlled biomass burn during from the FLAME-2 experiment. To our knowledge this is currently the fastest system for acquisition of chemically resolved aerosol data.



## 1. Introduction

Aerosols have important effects on climate, visibility, human health, as well as the transport and deposition of acid, toxic, acidifying and eutrophying pollutants. Characterization of these impacts requires a fundamental understanding of aerosol processes, chemistry, and microphysics. Great efforts are being made on each of these fronts, but progress is complicated by the rich chemistry, short lifetimes and highly variable spatial and temporal distributions of aerosols. Aerosol research thus demands analytical instrumentation capable of analyzing a diversity of chemical classes with broad dynamic range and high time resolution.

The time-of-flight aerosol mass spectrometer (ToF-AMS, Aerodyne Research, Billerica, MA) [1,2] is a field-deployable instrument, which is used primarily in atmospheric science laboratory studies and field campaigns. The instrument can acquire data in a particle time-of-flight (PToF) mode, where particle size and chemistry are simultaneously recorded, or in a more sensitive MS mode, where only average particle chemistry is recorded [3]. Typical data sets report ambient concentrations of submicron non-refractory aerosols (NR-$PM_1$) across periods of several hours to several weeks with data averaging times typically ranging from seconds to minutes. Recorded mass spectral signals are apportioned to total organic aerosols (OA) and non-refractory inorganic species using the "fragmentation table" approach [4] and/or direct processing of the high-resolution ion signals [2] and converted into mass concentrations based on instrument calibrations to generate time

* Corresponding author at: Dept. of Chemistry and Biochemistry & CIRES, University of Colorado, UCB 216, Boulder, CO 80309-0216, United States.
Tel.: +1 303 492 3557; fax: +1 303 492 1149.
*E-mail address:* jose.jimenez@colorado.edu (J.L. Jimenez).

1387-3806/$ – see front matter © 2010 Elsevier B.V. All rights reserved.
doi:10.1016/j.ijms.2010.12.004

series and size distributions of each species. Higher order data processing may involve elemental analysis of the OA [5,6] or positive matrix factorization of the OA spectra to separate the main sources/components [7].

The inherent time response limits of the ToF-AMS are approximately 100 Hz in PToF mode and 20 kHz in MS mode. The PToF-mode limit corresponds to the frequency of the particle gating chopper, whiles the MS-mode limit is determined by either the single particle evaporation time (~50 μs [8]) or the ion time-of-flight extraction frequency, which is typically between 20 and 80 kHz. Before the developments reported here, the ToF-AMS operated with a minimum save time of approximately 1 s in both the MS and PToF modes. The chemistry and microphysics of aerosol generation and processing can be extraordinarily dynamic, and many potential applications of the ToF-AMS require better time resolution. These include sampling of highly dynamic aerosol sources such as flames or internal combustion engines, measurements from aircraft or other moving platforms with high spatial resolution, direct quantification of chemically resolved aerosol emission and deposition fluxes with the eddy covariance (EC) technique, and fundamental study of particle vaporization inside the AMS.

Mobile laboratories such as instrumented aircraft, ships, and trucks are increasingly being used in atmospheric chemistry as way to probe the spatial distribution of emissions and chemistry. Often, signals of interest such as plumes from individual sources such as power plants or ships have narrow spatial extent and rapidly changing concentrations and structure. Characterization of these sources and their concentration profiles demands that analytical equipment have high temporal resolution. For example research aircraft operate at speeds from ~50 m/s (DeHavilland Twin Otter) to around 250 m/s (Gulfstream V) and previous ToF-AMS experiments have used time resolutions of ~10 s which translate into spatial resolutions of 0.5–2.5 km (e.g., [9]). Spatial resolutions down to a few meters are of interest but have not been previously achievable by aerosol chemical instrumentation.

A potentially exciting application of fast ToF-AMS acquisition is chemically resolved aerosol flux measurements using the EC technique. Emission and deposition of particles over ecosystems and urban environments remain highly uncertain due to a lack of measurements, but have important implications for particle sources and lifetime. Often emission and deposition are occurring simultaneously and thus total particle fluxes can be difficult to interpret [10]. For this reason chemically resolved particle flux measurements are a more powerful means to identify and quantify the different sources and processes. Particle number fluxes due to biogenic secondary organic aerosol (SOA) formation over forests have been reported [11], while ecosystem-relevant dry deposition of particulate nitrogen and sulphur has been measured by gradient methods [12,13]. EC measurements are the only direct approach to fluxes [14], but have stringent instrumental requirements—namely, sensitive, selective measurements of chemical species at 5–10 Hz for extended periods of time (30 min). Recently, a system for chemically resolved EC measurements using the quadrupole AMS has been demonstrated and used to quantify fluxes of inorganic species and organic components over an urban area [15], but due to the scanning nature of the quadrupole it can only report EC fluxes at ~10 discrete mass-to-charge ratios ($m/Q$). An improved system that can report fluxes across a broad $m/Q$ range, and thus of various organic and inorganic components, is highly desirable.

Time-of-flight mass spectrometers (TOFMS) are capable of measuring mass spectra at extremely high rates. For instance, a TOFMS run with an ion extraction frequency of 50 kHz performs a unique mass spectral measurement every 20 μs. But, total acquisition of a spectrum requires (i) measurement of ion times of flight and digitization of the data, (ii) transfer of the digitized data from the data acquisition electronics to the PC RAM, (iii) optional averaging or pre-processing of the data in PC RAM, and (iv) writing of the data to disk. Depending on the data acquisition electronics and PC employed, steps (ii) through (iv) often limit effective acquisition to rates much lower than the TOFMS extraction frequency.

The choice of PC data acquisition (DAQ) card for use with a TOFMS depends on the nature of the data being acquired. Signals in averaged TOF mass spectra can be divided into two classes: (i) low abundance, which have shape and intensity originating from the accumulation of stochastic single ion detection events and (ii) high abundance, which have shape and intensity originating from the accumulation of signals generated by the simultaneous detection of multiple ions. A common approach for quantification is pulse counting [16], where a time-to-digital converter (TDC) is used to record ion times of arrival. A histogram of arrival times is accumulated over successive TOFMS extractions, producing a mass spectrum with peak areas proportional to ion concentrations. TDC-based electronics record no information about the intensity of the instantaneous signals. Thus, TDCs are only quantitative in the low abundance regime, where recorded signals can be assumed to be produced by the arrival of single ions at the detector [17]. Determining the number of ions contributing to high abundance signals in TOFMS requires the use of an analog-to-digital converter (ADC), which digitizes signal waveforms from individual extractions in a manner that maintains information about both time of occurrence and amplitude.

In the ToF-AMS ions are detected in bursts following the rapid (typically 50 μs) vaporization and ionization of particles. Intense signals originating from the simultaneous detection of multiple ions are common. For instance, a pure 500 nm ammonium nitrate particle might generate ~30 $NO^+$ ions within each of five consecutive TOFMS extractions corresponding to the particle vaporization event, and this number grows as the cube of particle diameter. Such high count rates make ion counting with a TDC non-quantitative [18] (because the number of ions contributing to the recorded signal is ambiguous) and distort the measurement of peak positions [19,20] and therefore the accurate $m/Q$ measurement [21,22]. In order to quantify signals, the ToF-AMS uses an ADC-based DAQ card (detailed in a later section). This enables analysis with large dynamic range [23], but, because TOFMS data accumulated on the DAQ card are waveforms with tens of thousands of 16 or 32-bit values, rather than the 1-bit values of a TDC, the times required for data transfer, processing, and save significantly affect performance.

In an effort to expand instrument capabilities, the data acquisition routines of the ToF-AMS have been restructured with an emphasis on increased acquisition rates. In this paper we report the architecture of this new data acquisition model and the effects of key variables on performance. Demonstration results for several important applications are presented. Rates exceeding 1000 Hz are achieved for MS mode, demonstrating that this TOFMS can be used as a detector for fast chromatographic analysis of signals beyond the ion-counting limit. We characterize the advantages of a specific high-performance ADC-based DAQ card with current PC technology. With straightforward adjustments, this discussion can be applied to alternative TOFMS acquisition systems, and updated as improved ADC and PC technology become available in the future.

## 2. Methods

A general schematic of the ToF-AMS is shown in Fig. 1. Instrument details and characterization of key figures of merit for the different instrument variants and modes of operation can be found in DeCarlo et al. [2]. Ambient particles are sampled directly from atmospheric pressure into the instrument's vacuum system via an aerodynamic lens [24], which focuses particles into a tight beam.

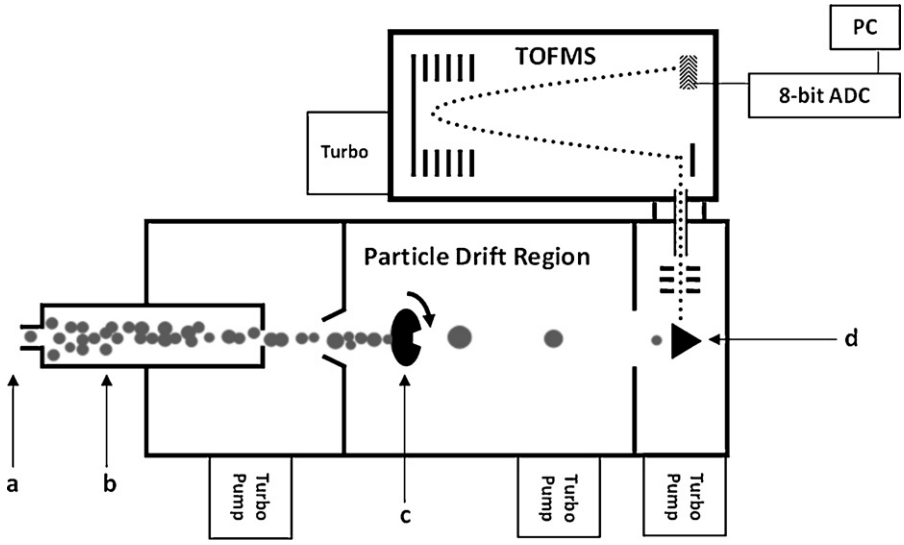


**Fig. 1.** Schematic of the ToF-AMS. Air is sampled from atmospheric pressure into vacuum through the sample inlet (a). Particles are focused into a beam by an aerodynamic lens (b) and travel across the particle flight chamber. Beam transmission to the vaporizer is determined by a rotating mechanical chopper (c), which can be positioned in a blocking, transmitting, or modulating position. Particles impact a conical heater (d) and are vaporized. The resultant gaseous plume is analyzed by EI-TOFMS. TOFMS signal waveforms are digitized and averaged by an ADC-based DAQ card.

Particle vacuum aerodynamic diameters are determined by modulating the beam with a mechanical chopper and measuring flight velocities across the first vacuum chamber. At the end of the particle flight region, particles impact a heated surface (typically 600 °C) which leads to vaporization of non-refractory species. The resultant plume of vapor is analyzed by electron ionization (EI) TOFMS. The ToF-AMS is built with either a compact or a high-resolution TOFMS (CTOF or HTOF platform, respectively) from Tofwerk AG (Thun, Switzerland). The HTOF can be operated in the high-sensitivity and medium-resolution "V-mode" ($m/\Delta m = 2500$) or the dual-reflectron "W-mode," which has higher resolution ($m/\Delta m = 5000$), but lower sensitivity. AMSs equipped with both TOF platforms were used in this work, and are referred to as the C-ToF-AMS and HR-ToF-AMS.

Typical particle flight times from the mechanical chopper to the vaporizer are 3–6 ms. In the PToF mode, multiple mass spectra (on the order of 100) are acquired across the duration of a single chopper cycle, and successive chopper cycles are averaged. The two-dimensional data set represents a quantitative measure of aerosol chemistry (MS axis) as a function of size (particle flight axis). For increased sensitivity, the instrument is also run in MS mode, where the particle beam is not modulated and averaged mass spectra are acquired for a higher fraction of sampled aerosols but without size resolution. In MS mode, the mechanical chopper is moved laterally between positions that block and transmit the entire gas and particle beam. The blocked measurements record the instrument background and are subtracted from the data acquired in the transmission position to yield a mass spectrum of aerosol components.

To allow quantification of signals, the ToF-AMS uses a DAQ card with an analog-to-digital converter (ADC) and FPGA-managed (field-programmable gate array) averaging functionality (Acqiris AP240, PCI module, Agilent, Geneva, Switzerland). Signals generated by the micro-channel plate detector of the TOFMS are sampled by the ADC at 1 GSample/s and digitized as 8-bit values. In MS Mode, data from successive TOFMS extractions are summed in the memory of the DAQ card to produce a single summed ("averaged") MS waveform. PToF mode employs the round-robin sequence averager mode of the AP240, in which the final data array contains a user-defined number of equal-length segments, each of which contains a summed mass spectrum. Acquisition of this data array is triggered by the chopper, indicating the start signal of the particle time-of-flight measurement, and the segment number of a mass spectrum has a linear correspondence to particle flight time. Successive chopper cycles are summed to generate an averaged PToF Mode data set.

Data averaging in both modes is managed by the FPGA of the AP240 and averaged waveforms are accumulated in the memory of the AP240, allowing the PC to conduct separate acquisition-related tasks (e.g., processing, display, or write to disk) simultaneous to data recording without multithreading. The advantages of this approach are discussed below. Summed values are transferred to the PC as 2 or 4 byte values, depending on the averaging time. Agilent specifies a maximum transfer rate of 100 MB/s to the host processor over the PCI bus. Critically, data acquisition is idle while the summed waveform is transferred from the DAQ card to the PC memory. Data in PC memory can undergo optional pre-processing before save to disk.

The ToF-AMS data acquisition software is written in Visual Basic.NET 2003 (Microsoft, Redmond, WA). Data are saved as Hierarchical Data Format Version 5 (HDF5) files (HDF Group, Champaign, IL, www.hdfgroup.org). Typically MS-mode data are saved as both a normalized ion time-of-flight waveform having units of signal intensity per TOF extraction and as a unit mass resolution (UMR) spectrum. The former is a raw waveform that can be mass calibrated in post processing and used for exact mass analysis, while the UMR spectrum contains summed data for regions centered on integer $m/Q$ values. PToF-mode data are typically saved only as UMR spectra to reduce data size in the hard disk, although save of raw data is available. For these experiments, there was no processing of data between transfer and save. Data saved in both modes were only the raw summed waveform transferred from the DAQ card.

Achievable data acquisition rates are characterized as a function of DAQ card and PC performance. Data transfer and save rates were determined by measuring processes using high-resolution timers (function *QueryPerformanceCounter*, MSDN Library, Microsoft) within the compiled code. Overhead parameters such as HDF file open and file close times were determined by measuring acquisition processes for data arrays of zero dimension. Achieved acquisition rates were calculated by comparing time stamps from successive data saves.

The HDF library includes functionality for real-time gzip compression (http://www.gnu.org/software/gzip/) with adjustable compression levels, having an inverse relationship between compression factor and effective write-to-disk speed. Achieved compression depends on the nature of the dataset. Unless otherwise noted, experiments in this work did not employ gzip compression.

The standard ToF-AMS PC is equipped with a single-core processor, and the ToF-AMS DAQ is written for use on such a PC (e.g., Intel Pentium 4, 2.80 GHz, 512 MB RAM). To demonstrate the advantage that can be gained by implementation of a multi-threaded data acquisition routine, we also characterize the performance achieved with the Tofwerk TofDaq data acquisition software running on a multicore processor (DELL Dimension 9200, Core2Duo E6400 CPU, 2 GB RAM, RAID0 disk). In TofDaq, communication with the DAQ card, real time processing of data, and save of HDF5 data to disk are all implemented in different threads. Data are downloaded into a ring buffer from where they can be continuously processed and saved to disk. Saving and processing thereby become asynchronous to recording and data acquisition becomes more independent of the saving to disk.

### 2.1. Fast MS mode (FMS)

For the standard MS Mode, a single data save ("run") contains data collected with the chopper positioned in both the beam-transmitting ("open") and beam-blocking ("closed") positions. The ratio of open/closed data is adjustable but is typically kept near 1:1. So, for instance, a 30-s run might be constructed by interleaving 5-s periods of open and closed acquisition. The chopper is moved using a servomotor (Hitec HS-81, http://www.hitecrcd.com), and the translation of the chopper can take hundreds of milliseconds. To avoid ambiguity about chopper position during data acquisition, there is a 100–500 ms break in acquisition after the initiation of any chopper movement. For save rates greater than 2 Hz, this chopper movement time can produce substantial inefficiency. A second consideration is the evaporation rates of the sampled species. Less volatile molecules may still be evaporating in the first second following the movement of the chopper from the open to blocked position [25]. As a consequence, short duration closed (background) data can contain significant contribution from some sampled aerosol species, leading to potential underestimation of species concentrations.

For the data presented here, the ToF-AMS uses a new Fast-MS (FMS) mode of data acquisition. In FMS mode, a given run contains only chopper-open or chopper-closed data, and data are acquired in cycles according to the following sequence: Block of Closed Runs – Block of Open Runs – Block of Closed Runs. For example, five closed runs, each of 1-s duration, may be acquired followed by thirty open runs, also each of 1-s duration, and so on. In this way, the chopper is only moved twice per cycle. The averaging time per run and the duration of the data blocks are user-adjustable. Difference spectra are calculated using an averaged closed spectrum that is determined by interpolation of data from the starting and ending blocks.

### 2.2. Eddy covariance measurements

The development of the FMS acquisition mode also enables EC flux measurements with the ToF-AMS. The need to correlate concentration measurements to fast measurements of the wind vector and the frequency-based analyses that need to be conducted on the EC data for quality control require that there is a precise period between successive mass spectra within a cycle. To achieve this, a modified version of the FMS routine has been developed, which triggers MS acquisition based on the PC internal clock. The standard flux cycle has a 30-min duration with closed and open block times of 30 s and 29 min, respectively. 95-ms average mass spectra are acquired and saved following a 100-ms timegrid with 5-ms precision. To achieve this precision, a timegrid is defined at the start of acquisition, where run $n$ of the cycle should begin at time $t = 0.100n$ s. If run $n-1$ does not finish in time for run $n$ to start between ($t = 0.100n$) and ($t = 0.100n + 0.005$) s, run $n$ is missed and the system prepares for run $n+1$. A valid flux cycle can miss no more than 0.55% of runs. Missed runs are interpolated in the post analysis and flux calculation. If a valid cycle cannot be achieved, the averaging time can be reduced while maintaining the 10-Hz time grid. This reduction increases the time available for data transfer and other PC processes (5 ms for 95 ms averaging). Simultaneous to the MS acquisition, the ToF-AMS acquisition software records wind speed, wind direction and temperature data from a sonic anemometer via a RS232 connection, which need to be recorded in a synchronized way for EC data processing [15]. The user has the option of saving the raw TOFMS data waveforms and/or UMR data. Additionally, the user may save data for custom defined $m/Q$ integration regions (for instance, a high resolution window centered on an exact $m/Q$).

### 2.3. Field campaigns

Data from two field experiments are presented to demonstrate the general FMS mode. The FLAME-2 (Fire Lab at Missoula Experiment, Phase 2) campaign was focused on quantification of emissions from controlled biomass burning experiments simulating wildfires, and was conducted at the United States Forest Service's Fire Science Laboratory in Missoula, Montana [26]. An HR-ToF-AMS was positioned on a platform 30 m above the burn and sampled air directly from the chimney stack. In the second experiment, an HR-ToF-AMS was installed aboard the NASA DC-8 research aircraft as part of the Arctic Research of the Composition of the Troposphere with Aircraft and Satellites (ARCTAS) field campaign [27].

EC flux data were acquired as part of the Biosphere Effects on Aerosols and Photochemistry Experiment, Phase 1 (BEARPEX-1) at the University of California Blodgett Forest Research Station [28]. Air was sampled from the top of a scaffolding tower through a 25-m, 1.27-cm O.D. copper line under turbulent flow to minimize smearing of the ambient concentration fluctuations. A sonic anemometer/thermometer (3D, Applied Technologies, Inc., Longmont, CO) located within 30 cm of the inlet recorded wind speed, wind direction and temperature at 20 Hz. Further experimental details are similar to those in Nemitz et al. [15].

## 3. New acquisition strategy

### 3.1. MS mode

As discussed earlier, the total acquisition of a TOFMS data file requires (i) digitizing and summing of data for successive TOFMS extractions on the DAQ card, (ii) transfer of the MS data from the DAQ card to the PC RAM, (iii) optional averaging or pre-processing of the data in PC RAM, and (iv) write of the data to disk. To maximize efficiency, FMS acquisition routines include only those processes that are necessary, and which cannot be accomplished in post-analysis. Calculations, such as the generation of UMR data or normalization of data values are not performed.

To help understand the advantages of the ToF-AMS acquisition system, consider a simple, optimized acquisition routine that follows a sequence where individual TOFMS extractions are recorded, transferred to RAM, and added to the average waveform. This sequence would repeat continuously, with acquisition stalled dur-

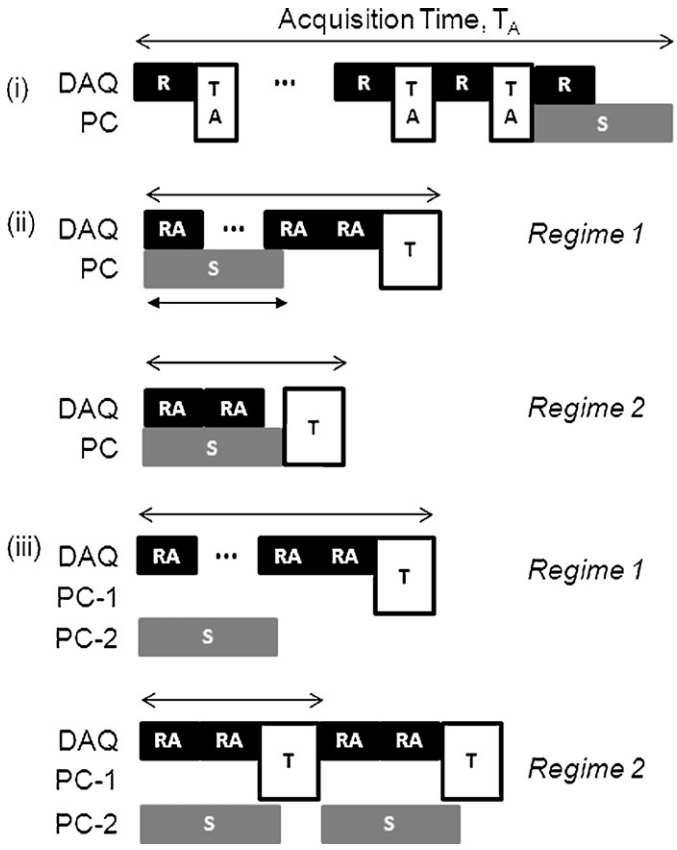


**Fig. 2.** Schematic timeline of DAQ card and PC management of TOFMS data acquisition tasks for (i) a sequential acquisition scheme, (ii) ToF-AMS DAQ (single thread) scheme and (iii) Tofwerk TofDaq (multi-thread) scheme. Included tasks are: (*R*) recording and digitizing a TOF extraction waveform. (*A*) Averaging/summing of successive extraction waveforms. (*T*) Transfer of data from the DAQ card to the PC RAM. (*S*) Save of averaged TOF extraction waveforms to the hard disk. For (ii) and (iii), summing of successive TOFMS extractions in the memory of the DAQ card reduces the transfer events/acquisition to 1 and allows the PC to save previously acquired data simultaneous to data recording. When considering total acquisition time, $T_A$, two regimes arise depending on the relative durations of the recording and save steps.

ing each transfer step, until the eventual save. Fig. 2 outlines how the DAQ card and PC manage TOFMS acquisition tasks for (i) the proposed sequential method, (ii) ToF-AMS DAQ (single thread) acquisition and (iii) Tofwerk TofDaq (multi-thread) acquisition. Specifically, we consider recording and digitizing a TOF extraction waveform (*R*), averaging/summing of successive extraction waveforms (*A*), transfer of data from the DAQ card to the PC RAM (*T*), and save of the averaged TOF extraction waveform to the hard disk (*S*).

In contrast to the sequential method, the ToF-AMS DAQ and TofDaq routines sum recorded TOF extractions in the memory of the DAQ card. For high rates, and while averager memory is not saturated, this on-board summing strategy reduces the number of card-to-computer transfers to 1 per save. For all three methods, data transfer requires the attention of both the DAQ card electronics and the PC and therefore represents a dead time in recording. Thus, reducing the number of transfer events can significantly improve acquisition efficiency.

The second advantage of methods (ii) and (iii) over the depicted sequential scheme (i) derives from the fact that the PC is free to manage separate tasks during the digitization and summation of successive TOF extractions. Where the sequential method initiates a save after the transfer of the final TOFMS extraction waveform and pauses data recording during the save event, methods (ii) and (iii) save previously recorded data simultaneous to recording and summing of new data by the DAQ card. This simultaneous save strategy is not possible in the sequential scenario (i), because the duration of a single TOF extraction recording event is much shorter than the time required to write to disk, and the PC must be done with saving before it can handle the next transfer event.

The depiction of the ToF-AMS DAQ acquisition method in Fig. 2(ii) can be used as a starting point for predicting achievable acquisition rates. The total time required for acquisition of an averaged data file ($T_A$) is a function of the time spent recording successive TOFMS waveforms ($T_R$) (summing of successive waveforms by the DAQ card is treated as instantaneous), the time required to transfer the averaged waveform from the DAQ card to the PC RAM ($T_T$) and the time required to save the average waveform from PC RAM to the PC hard disk ($T_S$). (The supplemental materials include a table defining all variables.)

The data recording time, $T_R$, is a user adjustable parameter, which determines the temporal resolution of the measurement. $T_R$ can be written as a function of the TOF extraction frequency ($F_{TOF}$) and the number of successive TOF extractions averaged per save, *N*:

$$T_R = \frac{N}{F_{TOF}} \tag{1}$$

For long $T_R$, total acquisition ($T_A$) is approximately equal to $T_R$. This work focuses on acquisition for fast applications which require short $T_R$, where the time necessary for data transfer and data save contribute significantly to the total acquisition time.

The time required to transfer data from the DAQ card to the PC ($T_T$) and $T_S$ are functions of the number of data points recorded ($p$) per spectrum, the size of each data point in bytes ($b_T$ and $b_S$, for transfer and save, respectively), the rate at which data are transferred ($F_T$), and the rate at which data are written to the PC hard disk ($F_S$). For fixed $p$, $b_T$ and $b_S$, both transfer time and save time are

independent of recording time:

$$T_T = \frac{pb_T}{F_T} + K_T \quad (2)$$

$$T_S = \frac{pb_S}{F_S} + K_S \quad (3)$$

$K_T$ and $K_S$ are constants representing the time needed for overhead processes in the transfer and save events.

As shown in Fig. 2, two acquisition regimes arise, depending on the relative durations of data recording and data save. In regime 1, the defined duration of data recording on the DAQ board is greater than the time required to save the previously acquired data values to disk. Data are saved in parallel at no expense to efficiency, and total acquisition time is the sum of the recording time and the transfer time:

$$T_{A,\,Regime\,1} = T_R + T_T \quad (4)$$

Reduction of recording time eventually leads to regime 2, where recording time is shorter than the save time. Total acquisition time is then independent of $T_R$ and is fixed at a minimum achievable value that is the sum of $T_S$ of $T_T$:

$$T_{A,\,Regime\,2} = T_S + T_T \quad (5)$$

Decreases in $T_R$ have no effect on the achieved acquisition rate, suggesting that there is no reason to acquire data with $T_R < T_S$. The point at which the system transitions from regime 1 to regime 2, which is the maximum achievable acquisition rate ($F_{A\,max}$) can be calculated as:

$$F_{A\,max} = \frac{1}{T_S + T_T} \quad (6)$$

For any high-speed measurement, in addition to the acquisition rate it is critical to also consider the efficiency of data collection. A common metric for efficiency is "duty cycle" ($D$), which is defined the fraction of active acquisition time that is spent recording data:

$$D = \frac{T_R}{T_A} \quad (7)$$

For ToF-AMS acquisition in regime 1 the duty cycle $D$ becomes

$$D_{Regime\,1} = \frac{T_R}{T_R + T_T} \quad (8)$$

At slower rates, where $T_R \gg T_T$, duty cycle is near 1. As $T_R$ is reduced, $T_T$ begins to represent a larger fraction of total acquisition time and duty cycle is significantly decreased. Eventually, $T_R < T_S$ (regime 2), and $T_A$ becomes a constant. Reductions in $T_R$ reduce duty cycle with no effect on achieved acquisition rate:

$$D_{Regime\,2} = \frac{T_R}{T_T + T_S} \quad (9)$$

The on-board summing of successive TOF waveforms by the DAQ card reduces the number of DAQ-card-to-PC-RAM transfer events, and thereby enables high duty cycle acquisition. In the supplemental materials, we quantify the benefit of this continuous averaging by comparison to the hypothetical sequential scenario. For the ToF-AMS using the Acqiris AP240 DAQ card, the calculated improvement in duty cycle over a similar card without onboard averaging is approximately the ratio of the magnitudes of the digitizing and transfer rates. For digitization at 1 GS/s and a quoted transfer rate of 100 MB/s, this equates to approximately a factor-of-10 improvement. It should be noted that a similar advantage can be achieved with digitizers that use multiple memory banks and ping pong methods, where acquired data are written to a one memory bank while previously recorded data are transferred from another.

Fig. 2 also depicts the multithreading routines of the Tofwerk TofDaq acquisition software. Critically, the PC handles data transfer and data save on independent threads ("PC-1" and "PC-2"). Visual inspection of Fig. 2 shows that this offers no advantage in regime 1: for fixed $T_R$, $T_A$ is equal to that of ToF-AMS DAQ. But, in regime 2, where $T_R < T_S$ and the acquisition rate of the ToF-AMS DAQ is a constant, $T_A$ for TofDaq continues to be the sum and $T_R$ and $T_T$, such that reductions in recording time to lead increased acquisition rates. This point will be re-visited in Section 4.1.

### 3.2. PToF mode

This algebraic model is easily extended to the ToF-AMS PToF mode. As detailed earlier, the final PToF data set is a two-dimensional matrix having a user-defined number of rows, $r$, each of which is a unique mass spectrum having $p$ data points. Following each particle time-of-flight measurement start trigger, a block of $r$ unique mass spectra is acquired. Whereas in MS mode, the DAQ card acquires and sums successive mass spectra, in PToF mode it acquires and sums $N_{Chop}$ successive $r \times p$ data blocks (chopper cycles). From the standpoint of the acquisition system, the summed data block is the equivalent of an MS array of length equal to the product $rp$. Substitution into Eqs. (2) and (3) yields:

$$T_{T,PToF} = \frac{rpb_T}{F_T} + K_T \quad (10)$$

$$T_{S,PToF} = \frac{rpb_S}{F_S} + K_S \quad (11)$$

Because the system does not demand that TOF data are acquired continuously across the complete period between successive chopper start triggers, the PToF recording time, $T_{R,PToF}$, cannot be calculated as a function of TOFMS parameters. Instead, $T_{R,PToF}$ is a function of the chopper frequency, $F_{Chop}$, and the number of choppers averaged per save, $N_{Chop}$:

$$T_{R,PToF} = \frac{N_{Chop}}{F_{Chop}} \quad (12)$$

This definition of $T_{R,PToF}$ can be substituted above for consideration of operating performance (e.g., regime 1 versus regime 2) and duty cycle.

## 4. Results

### 4.1. Achievable rates

Fig. 3a compares the achieved ToF-AMS acquisition rates ($F_A$) for a 10,000 sample mass spectrum acquired with varied recording time ($T_R$) to the rates estimated using the equations in the previous sections. $T_A$ was calculated for regimes 1 and 2 using Eqs. (4) and (5). Transfer and save rates were measured to be $F_T$ = 100 MB/s and $F_S$ = 150 MB/s, with overhead times of $K_T$ = 170 μs per transfer and $K_S$ = 230 μs per save event. The calculated rates using each equation are shown as dashed lines. The point where these two lines cross determines the boundary of regimes 1 and 2, which is the ToF-AMS DAQ max achievable acquisition rate. Measured data rates for the ToF-AMS DAQ, shown as triangle markers, track the model closely in regime 1, where recording time ($T_R$) is greater than save time ($T_S$). Decreases in $T_R$ lead to increases in achieved acquisition rate. And, as predicted by the algebraic model, the achieved acquisition rate plateaus at approximately 1350 Hz for all values of $T_R$ less than or equal to $T_S$ (regime 2). In addition to characterizing current performance limits, this model should allow us to predict performance improvements enabled by future advances in DAQ electronics and PC hardware.

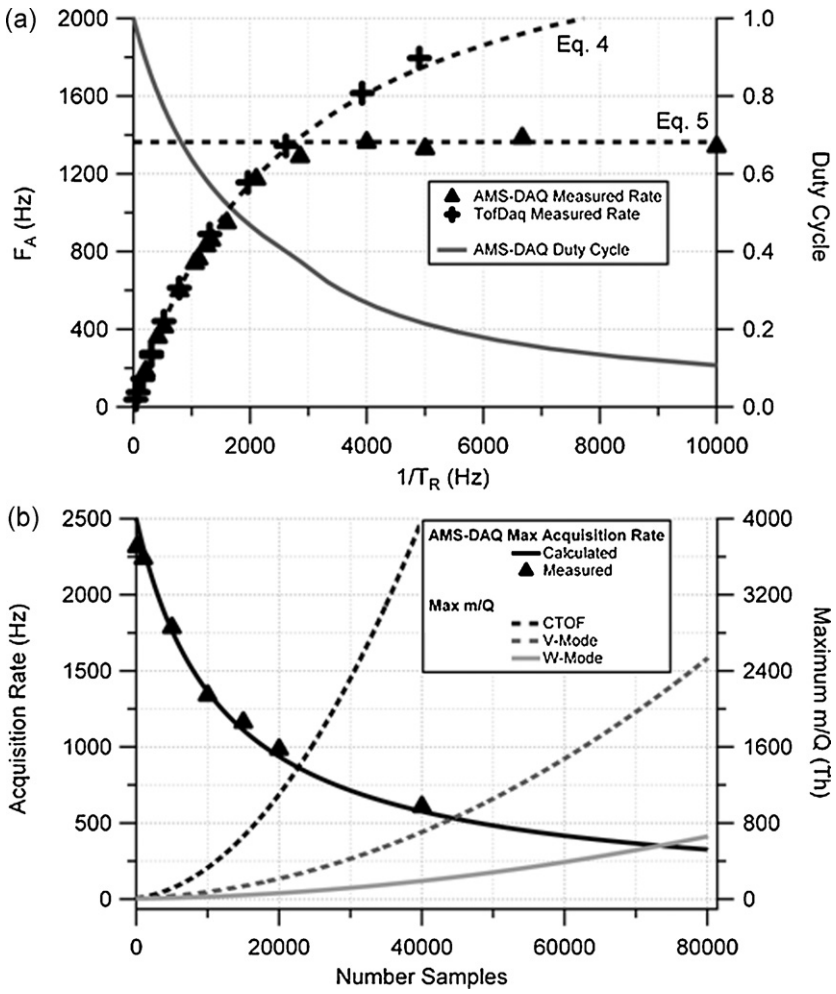


**Fig. 3.** (a) Comparison of the effective performance of the ToF-AMS for a 10,000 sample mass spectrum to the expected performance with measured rates and overhead co-efficients. Dashed lines show the anticipated performance based on Eqs. (4) and (5). $F_{A\,Max}$ ToF-AMS is approximately 1350 Hz. Data collected with the TofDaq software exceed this limit, demonstrating the advantage of multithreaded data acquisition software routines. (b) Maximum achievable acquisition rate, $F_{A\,Max}$, for the ToF-AMS as a function of the number of samples recorded (Eq. (6)). The right axis shows the upper $m/Q$ value detected with the CTOF, V-mode, and W-mode ToF-AMS configuration.

Also shown are data for Tofwerk's TofDaq recording software run under the same conditions. In regime 1, where $T_R > T_S$, achieved acquisition rates are effectively equal to those of the ToF-AMS DAQ. Beyond the regime 2 transition, where the ToF-AMS DAQ rate plateaus, the acquisition rate of ToFDaq continues to increase following Eq. (4). This difference is explained by the schematic in Fig. 2, which shows that download of data from the DAQ card to PC RAM is not delayed in any way by saving the data to disk, because the two processes are managed by separate PC threads. Thereby, data acquisition becomes completely independent on the saving to disk, and data acquisition rates are only limited by the recording time $T_R$ and data transfer time $T_T$. Discussion in the remainder of this paper will characterize performance of acquisition using the ToF-AMS DAQ, reflecting the standard hardware and software configuration on all ToF-AMS instruments worldwide. Performance similar to that of the TofDaq software would be achievable by reprogramming of the ToF-AMS data software, although this is a complex task which is not justified at present.

ToF-AMS duty cycle ($T_R/T_A$) for the calculated rate line is plotted on the right axis of Fig. 3a. For this configuration, duty cycle is 0.99 at 10 Hz and 0.88 at 200 Hz. These high duty cycles are possible because idle time due to transfer events is minimized by summing of data in the memory of the ADC. Based on the derivation in the supplemental materials, duty cycle at 200 Hz would be approximately 0.088 for an equivalent system that was transferring each TOF extraction to the PC RAM independently (sequential strategy). Because transfer and save times in this system are independent of recording time, duty cycle decreases with decreased recording time. Fig. 3a clearly emphasizes the counter-productivity of reducing recording time in regime 2: duty cycle is decreased while achieved acquisition rates remain constant. If maximum acquisition rate is desired, the ToF-AMS should be run at the point where performance transitions from regime 1 to the regime 2 plateau. Specifically, this is the point where $T_R = T_S$.

Fig. 3b shows the maximum achievable MS acquisition rate for the ToF-AMS as a function of the number of samples in the mass spectrum, $p$. Values calculated with Eq. (6) and the measured transfer and save rates agree well with experimentally determined maximum rates. For any TOFMS, the number of samples acquired will determine the range of $m/Q$ values in the mass spectrum. Fig. 3b also plots the maximum $m/Q$ value recorded versus number of samples for the three TOFMS configurations of the ToF-AMS with standard tuning and timing. For typical ambient experiments, ToF-AMS data are collected with a $m/Q$ range extending to 400 Th. For such a configuration, the C-ToF-AMS can acquire data at approximately 1300 Hz, while the HTOF can acquire data at 700 Hz and 400 Hz, in V- and W-modes, respectively.

Fig. 4 displays calculated and measured PToF-mode performance for an instrument configured with $p = 10{,}000$ samples/spectrum (as in Fig. 3a), a chopper frequency of 100 Hz,

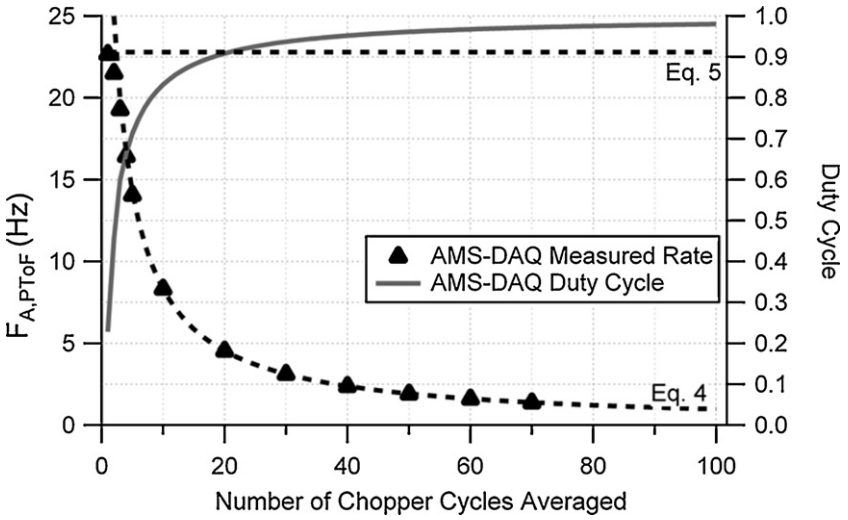


**Fig. 4.** Estimated PToF Mode performance calculated using the algebraic model (Eqs. (4) and (5)) a data block having $r = 100$ mass spectra and $p = 10{,}000$ samples/spectrum and a chopper frequency of 100 Hz. Data are plotted as a function of the number of chopper cycles averaged, $N_{chop}$. Achieved data rate (triangles) closing agree with calculated values, with a maximum rate of 22.5 Hz. Duty cycle is greater than 80% for rates below 10 Hz.

and 100 mass spectra per chopper cycle, $r$. (Note that displayed results are valid for conditions with this chopper frequency and $rp = 1{,}000{,}000$.) Data were saved in a raw format with no processing. The save rate in these experiments was determined to be $F_S = 80$ MB/s. Acquisition rates are plotted as a function of the number of chopper cycles summed per save, $N_{Chop}$. At these high acquisition rates, all summing is done in the AP240 memory, so that each save has only one transfer event. Again, achieved performance agrees well with that predicted by the algebraic model. The fastest possible PToF acquisition corresponds to the recording and storage of data for 1 chopper cycle. For these conditions, single chopper acquisition corresponds to approximately 22 data saves/s. In a perfectly efficient system, data would be recorded for every chopper and the achieved acquisition frequency, $F_{A,PToF}$, would be the chopper frequency divided by the number of choppers averaged. Because some chopper cycle triggers are missed during the data transfer step (and data save step in regime 2), achieved rates are lower than this value. The ratio of the achieved rate over the ideal rate is the duty cycle, which is plotted here for the calculated values. Notably, the system has duty cycle > 80% up to approximately 10 Hz ($N_{Chop} = 8$). Duty cycle falls rapidly past this point, as the system transitions from acquisition regime 1 to regime 2. These results suggest that an efficient EC PToF flux mode could be implemented, however the removal of particles by the chopper would greatly worsen statistics related to the effective sample size.

The enormous data load inherent to fast PToF mode acquisition limits the practicality of its implementation. Saving 2 byte values, the data load in this experiment is 2 MB/save (2.4 GB/min at 20 Hz) Some improvement can be achieved using the gzip compression. The achieved compression factor and the effect of compression on the achieved acquisition rate depend on nature of the data set. For example, tests of gzip with these experimental settings resulted in a factor of 5 decrease in file size with no loss of speed for rates less than 8 Hz (regime 1, where save time can increase without cost) and a factor of 10 decrease in file size for a 1-chopper experiment with a reduction in achieved rate from 22 to 14 Hz.

As a demonstration of the ability to resolve rapid, transient processes, Fig. 5 displays the $N_2^+$ signal ($m/Q$ 28) from the ionization of air molecules as the mechanical chopper is moved from the closed to the open and then back to the closed position. Data are presented for recording times, $T_R$, of 0.095 s, 0.0095 s, and 0.0005 s (Fig. 5a–c, respectively). The effective acquisition rate for each spectrum was calculated by comparison of successive timestamps. Average acquisition rates for the three cases were: 10.000 Hz, 93.1 Hz, and 1010 Hz. As mentioned earlier, achievement of acquisition on a precise time grid is critical for EC flux applications. The right axis shows the instantaneous acquisition rate for each save. As could be expected, the acquisition rate fluctuates more drastically as averaging time is decreased and the system becomes more susceptible to variations in processing times and latencies associated with other operating system tasks. Notably, for the 0.095 s data, standard deviation in acquisition rate is 8 ppm of the average. Even when letting the system run freely, a highly precise time grid is achieved at rates suitable for EC flux measurements with an effective duty cycle of 95%. During flux operation, a strict time grid is enforced by software timers.

From the two faster data sets, we can estimate that physical movement of the chopper between open and closed positions takes approximately 20 ms. Deviation in acquisition rate due to the issuing of the software command for chopper movement is clearly visible in the 0.095 s and 0.0095 s data. Most interesting are the outliers at 0.511 s and 1.01 s in the 0.0095 s data. Each is approximately 100 ms before the $N_2^+$ data indicate physical movement of the chopper. The command to move the chopper originates from the data acquisition software and the deviation in the rates of these two saves are assumed due to the processing of the command. In standard MS mode, user adjustable acquisition delays after chopper movement help avoid ambiguity in MS data collected just after calls for chopper transitions. For FMS mode, data post-processing routines usually ignore the data for saves taking place within 200 ms of a transition.

As mentioned, data load currently dissuades routine use of the fast PToF mode. To demonstrate its possible utility, functionality was added to the acquisition routine which calculated and saved chemically speciated size distributions, using simplified fragmentation tables [4]. For instance, a two-dimensional $m/Q$ versus particle size matrix is converted to a nitrate concentration versus particle size array by summing those components of the mass spectrum that represent nitrate ions. These data are then saved in place of the raw matrix. Achievable rates are reduced because of the addition of a calculation step, which turns out to be slower than the raw data save (the factor of reduction depends on the calculations implemented). Fig. 6 shows an example of a size-resolved nitrate time series. Ammonium nitrate particles were generated using a Collison atomizer (TSI 3076, St. Paul, MN) size-selected by passage through a scanning mobility particle sizer (TSI 3081) and sampled

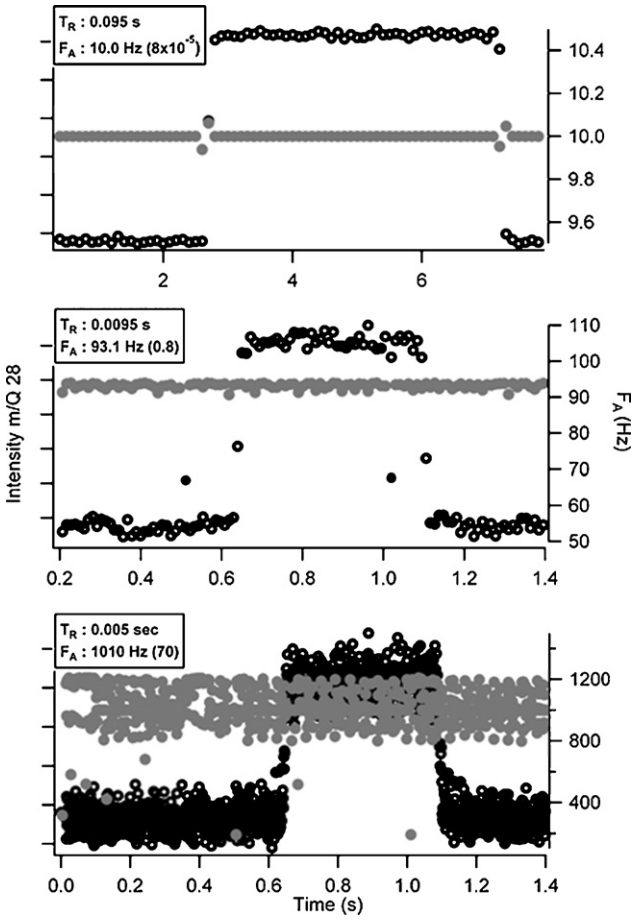


**Fig. 5.** To demonstrate monitoring of a rapidly changing system, mass spectra were acquired continuously while the mechanical chopper was moved latterly from the blocked to open to blocked position. When in the blocked position, the chopper reduces both gas phase and particle signals. The resultant $N_2^+$ signal (28 Th) is displayed, with acquisition at three rates. (a) $T_R$ = 0.095 s, (b) $T_R$ = 0.0095 s and (c) $T_R$ = 0.0005 s. The effective data acquisition rate for each save is also shown (right axis).

with the ToF-AMS which was acquiring PToF data at 5 Hz. The band pass of the SMPS was increased manually from 200 nm to 500 nm to change the sampled size distribution. This "growth" is clearly visible in the size-resolved nitrate data.

For these experiments, particles were generated at concentrations much greater than what are typical in ambient measurements, in order to demonstrate the size resolution at high acquisition rates. To measure changes in particle chemistry at high rates, where only a few chopper cycles are averaged per save event, a minimum of 10 particles should be present in every measurement to ensure good particle statistics. For a standard AMS chopper spinning at 100 Hz and having with 2% duty cycle and an acquisition rate of 5 Hz, this suggests a minimum practical aerosol concentration of 5000 particles $s^{-1}$ (3300 particles $cm^{-3}$ within the transmission range of the AMS.). Below this concentration, fast PToF measurements transition into a stochastic, near single-particle measurement regime. In addition, the particles need to carry sufficient mass to also satisfy the mass-based detection limit. For ammonium nitrate we can estimate the mass-based detection limit by scaling the value reported for MS mode [2] (1.2 ng $m^{-3}$ in 1 min. for the C-ToF-AMS) to the PToF mode at 5 Hz, which yields 1.6 μg $m^{-3}$. Thus the ambient concentrations will need to be substantially larger than that value for meaningful fast size distributions.

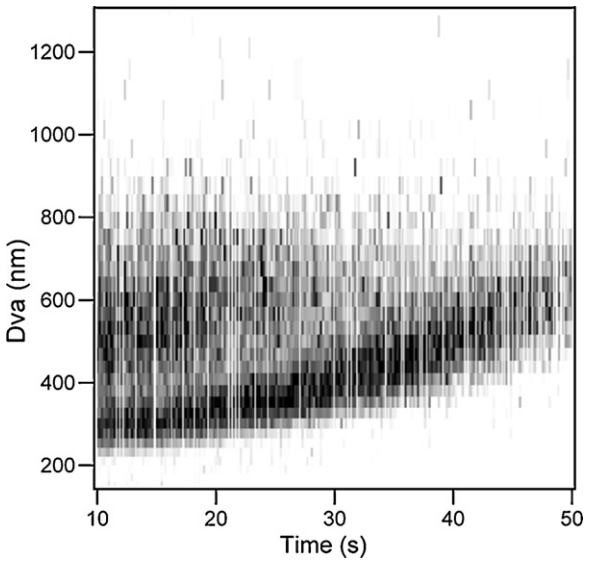


**Fig. 6.** Size-resolved time series of aerosol nitrate mass generated with 5 Hz PToF Mode acquisition. Ammonium nitrate particles presented to the ToF-AMS were size selected by manually tuning the band pass of a DMA connected upstream of the ToF-AMS over the 1 min time range presented.

### 4.2. Ambient applications

Fig. 7 demonstrates two applications of the FMS mode for real-time aerosol analysis. Fig. 7a shows total ToF-AMS organic aerosol signal for a controlled biomass burn during the FLAME-2 campaign. For biomass studies, highly time-resolved data allow the clear separation of the flaming and smoldering burn phases, as well as detailed evaluations of the relationships between PM emissions and those of gas-phase species which can also be measured at fast rates. MS data were collected with an HR-ToF-AMS in W-Mode. Trends in the 10-Hz ToF-AMS data agree well with the 1-Hz concentration data reported simultaneously by the DustTrak nephelometer (TSI) while the high-resolution 10-Hz mass spectra show good signal-to-noise (Fig. 7 inset), demonstrating the ability of the ToF-AMS to observe dynamic changes in aerosol chemistry at these rates. FMS data are saved in a raw format that is compatible with the well established routines for high-resolution ion fitting based on ToF-AMS data. As an example of this power, the inset shows a section of data near $m/Q$ 43 from a single 10-Hz mass spectrum, where $C_2H_3O^+$ is clearly resolved from $C_3H_7^+$ ($m/\Delta m \sim 4300$).

Fig. 7b demonstrates an application of the FMS mode aboard a moving laboratory platform, where acquisition rates translate linearly to spatial resolution. The 1-Hz time-series of AMS organic mass and sub-micron aerosol scattering recorded by the NASA Langley nephelometer were measured on the NASA DC-8 research aircraft during the ARCTAS campaign. The AMS mass loadings are shown shaded to clearly highlight the blocks of open/closed chopper positions; in the gaps the instrument measures an average background spectrum, which is interpolated across the shaded regions, where the total spectrum, including the particle beam is monitored. The figure shows the resulting mass concentration calculated from the difference spectrum for the "chopper open" periods. The time period shown reflects a single crossing of a boreal forest fire plume made by the DC-8 on July 1st, 2008; the low atmospheric background concentrations dramatically, and rapidly, increase and decrease on entering and leaving the plume. Within the plume, mass concentration changes of an order of magnitude are observed in a time scale of only a few seconds are well captured by the FMS acquisition mode; the nephelometer actually appears to

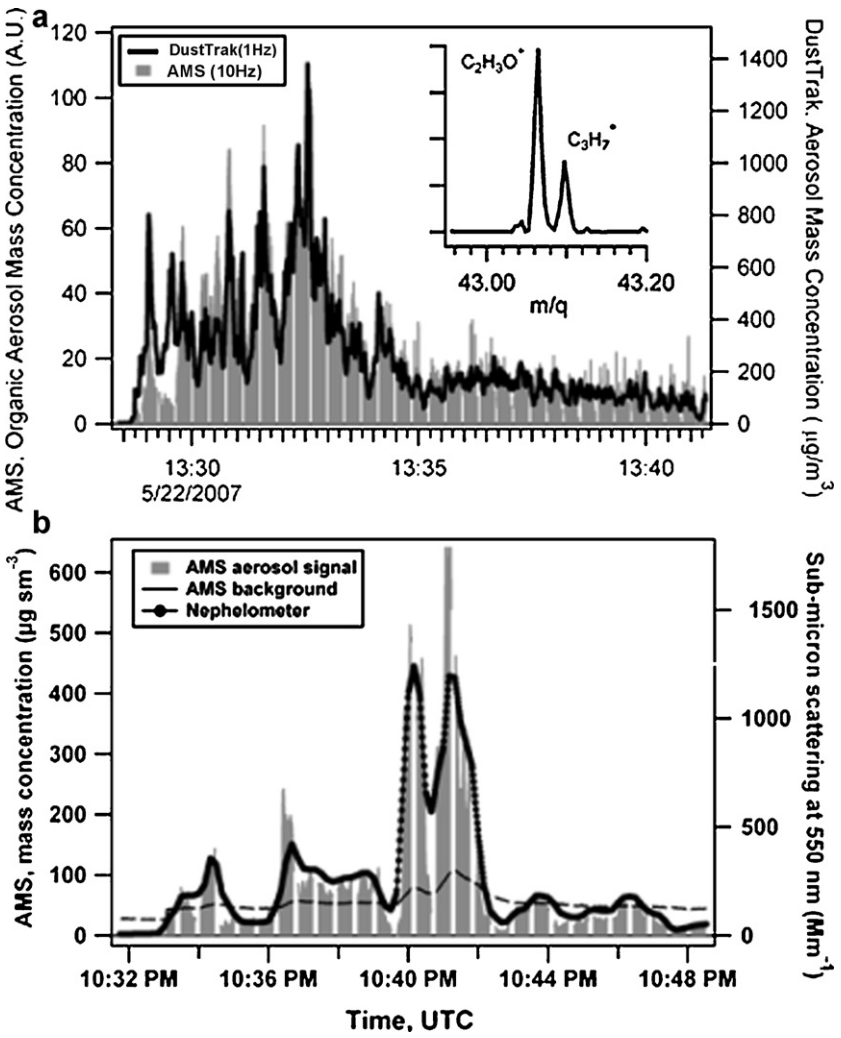


**Fig. 7.** (a) W-Mode HR-ToF-AMS monitoring of a controlled biomass burn during the FLAME-2 campaign. 10 Hz time series of total aerosol organic mass are compared to 1 Hz time series from a TSI DustTrak. Correlation demonstrates the ability of the ToF-AMS to monitor rapid changes in aerosol concentration and chemistry. (b) 1 Hz time-series of AMS organic mass and sub-micron aerosol scattering recorded by the NASA Langley nephelometer aboard the NASA DC-8 research aircraft crossing a boreal forest fire plume during the ARCTAS campaign. The AMS mass loadings are reported for the shaded areas, between which the instrument measures an average background spectrum. Mass concentration changes of an order of magnitude are observed in a time scale of only a few seconds.

have a slightly slower response to mass concentration changes but clearly verifies the AMS mass concentration trend. The standard method of AMS acquisition, with save times of order 10 s, would give only two data points for each shaded region; it is clear that this would incur a significant penalty in capturing the temporal and spatial dynamics of the smoke plume.

The utility of any fast measurement will depend on the sensitivity of the technique and the concentration of analytes being measured. Both of the FMS datasets displayed in Fig. 7 were acquired in direct proximity of a flame source, where aerosol concentrations can approach 1 mg m$^{-3}$. AMS measurements are more often made in polluted urban areas, where OA concentrations are typically in the range of 5–20 μg m$^{-3}$. The 1-min detection limit of the ToF-AMS for organic aerosol (OA) is 22 ng m$^{-3}$ (HTOF, V-mode) [2]. Scaling by the square root of averaging time suggests a 10-Hz detection limit of approximately 500 ng m$^{-3}$, which is adequate for acquisition in urban conditions. Recently, Farmer et al. [29] have applied the FMS acquisition mode to eddy covariance flux measurements (see next section), and have demonstrated sufficient sensitivity for 10-Hz acquisition in forests having OA concentrations on the order of 1.5–3 μg m$^{-3}$.

### 4.3. Eddy covariance flux measurements

As described above, EC flux measurements require detection techniques that are both sensitive and fast enough to capture the relevant fluctuations in concentration carried by turbulent eddies, and that can be run continuously for at least 30 min in remote field conditions. Field data from the BEARPEX campaign successfully demonstrates that the FMS mode of the ToF-AMS meets these requirements. The instrument maintained time-gridded 10-Hz acquisition as described above for half-hour segments alternating with half-hour lower time-resolution concentration and PToF measurements. The spectral density function of the co-variance between the vertical wind component and the high resolution signal taken for a single integer mass can be used to demonstrate that the ToF-AMS data are collected both sufficiently fast and for long enough to capture the relevant turbulent structure. Fig. 8 shows the cospectrum for $m/Q$ 46 for a single half-hour of fast data collected between 12 and 12:30 pm on 15 September 2007. The flux is derived from the integral of the cospectrum; for the individual half-hour presented in Fig. 8, a downward flux is calculated, corresponding to a flux of −1.04 ng/m$^2$/s, and a deposition velocity

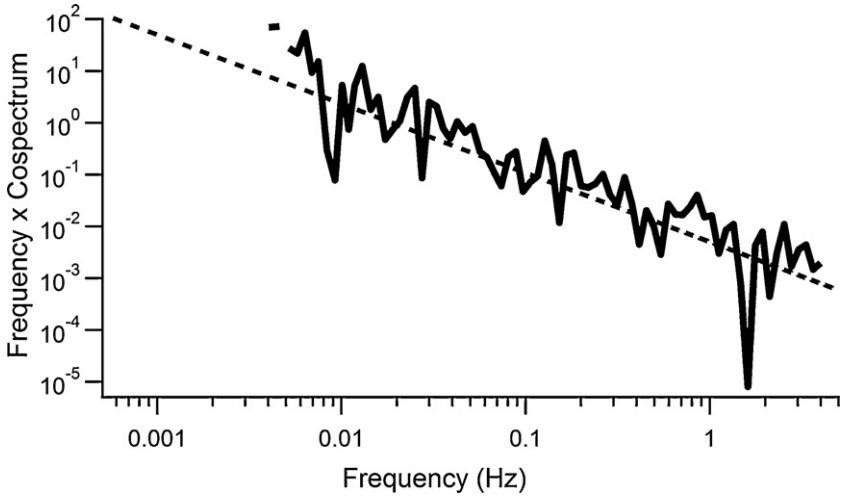


**Fig. 8.** Frequency-multiplied cospectrum of the vertical wind component (m/s) from the sonic anemometer and signal from the 46 Th fragment ($NO_2^+$) from the AMS for a single half hour (12:00–12:30 pm, 15 September 2007) during the BEARPEX campaign. The black line is the absolute value of the average cospectrum, binned by frequency. The dashed line shows the theoretical Komolgorov slope (−4/3), indicating the inertial subrange.

(-Flux/Concentration) at $m/Q$ 46 of 0.92 mm/s. Analysis of high resolution mass spectra shows that the peak at $m/Q$ 46 is dominated by the $NO_2^+$ ion, and can thus be considered representative of nitrate. This figure is typical of the daytime cospectra acquired during the BEARPEX campaign for dominant masses. The binned data, shown in black on Fig. 8, has a slope similar to that of the theoretical Komolgorov slope (−4/3, dashed line) derived for the inertial subrange for the flux-carrying eddies in the atmosphere, indicating that the instrument is capturing the relevant eddies. Acquiring fast data by ToF-AMS addresses a key need in the biosphere-atmosphere interactions community for chemically resolved particle flux measurements. Diagnostics of eddy covariance flux measurements, and details of their analysis and interpretation, are described in detail in a forthcoming manuscript [29].

## 5. Conclusions

A strategy for acquiring aerosol mass spectrometric data with time resolutions exceeding 1 kHz while maintaining high duty cycle has been demonstrated by optimizing the coupling of the PC software and the on-board summing operation of the ADC-based data acquisition card. Coupled aerosol size and MS measurements can be made at approximately 20 Hz. These rates are about 1/10 of the physically meaningful limits imposed by the ToF-AMS design. The fundamentals of the data acquisition system are discussed by means of a simple algebraic model. This discussion can easily be adapted and/or quantified for other TOFMS systems, and updated as newer computer-ADC systems become available in the future. The approach is based on performing the saving and acquisition tasks in parallel. With a single-thread code a ceiling rate of about 1 kHz is reached when the saving time becomes longer than the data recording time, but multithreaded code allows acquiring at even higher rates approaching 2 kHz with this system. Several applications of the new system have been demonstrated, including the measurement of rapidly changing aerosol sources, aircraft measurements with very high spatial resolution, and direct measurement of aerosol emission and deposition fluxes with the eddy covariance technique. High-mass resolution is retained in these applications. To our knowledge this is by far the fastest current system for acquisition of chemically resolved aerosol data.

## Acknowledgements

We thank B. Anderson (NASA) and A. Weinheimer (NCAR) for providing data from the ARCTAS project, C. Wold, W.-M. Hao, B. Malm, S. Kreidenweis, J. Collett, and their research groups for organization and logistical support during FLAME-2, and A. Goldstein, R. Cohen, and their groups, as well as Ken Docherty for support during BEARPEX-1. This work was partially supported by grants UCAR S05-39607 (HIAPER), NSF ATM-0513116 and ATM-0919189, NASA NNX08AD39G, EPA STAR-R833747, and NOAA OGP NA08OAR4310565.

## Appendix A. Supplementary data

Supplementary data associated with this article can be found, in the online version, at doi:10.1016/j.ijms.2010.12.004.

## References

[1] F. Drewnick, S.S. Hings, P.F. DeCarlo, J.T. Jayne, M. Gonin, K. Fuhrer, S. Weimer, J.L. Jimenez, K.L. Demerjian, S. Borrmann, D.R. Worsnop, A new time-of-flight aerosol mass spectrometer (ToF-AMS)—instrument description and first field deployment, Aerosol Sci. Technol. 39 (2005) 637–658.
[2] P.F. DeCarlo, J.R. Kimmel, A. Trimborn, M.J. Northway, J.T. Jayne, A.C. Aiken, M. Gonin, K. Fuhrer, T. Horvath, K.S. Docherty, D.R. Worsnop, J.L. Jimenez, Field-deployable, high-resolution, time-of-flight aerosol mass spectrometer, Anal. Chem. 78 (2006) 8281–8289.
[3] M.R. Canagaratna, J.T. Jayne, J.L. Jimenez, J.D. Allan, M.R. Alfarra, Q. Zhang, T.B. Onasch, F. Drewnick, H. Coe, A. Middlebrook, A. Delia, L.R. Williams, A.M. Trimborn, M.J. Northway, P.F. DeCarlo, C.E. Kolb, P. Davidovits, D.R. Worsnop, Chemical and microphysical characterization of ambient aerosols with the aerodyne aerosol mass spectrometer, Mass Spectrom. Rev. 26 (2007) 185–222.
[4] J.D. Allan, H. Coe, K.N. Bower, M.R. Alfarra, A.E. Delia, J.L. Jimenez, A.M. Middlebrook, F. Drewnick, T.B. Onasch, M.R. Canagaratna, J.T. Jayne, D.R. Worsnop, Extraction of chemically resolved mass spectra from Aerodyne aerosol mass spectrometer data, J. Aerosol Sci. 35 (2004) 909–922.
[5] A.C. Aiken, P.F. DeCarlo, J.L. Jimenez, Elemental analysis of organic species with electron ionization high-resolution mass spectrometry, Anal. Chem. 79 (2007) 8350–8358.
[6] A.C. Aiken, P.F. DeCarlo, J.H. Kroll, D.R. Worsnop, J.A. Huffman, K. Docherty, I.M. Ulbrich, C. Mohr, J.R. Kimmel, D. Sueper, Q. Zhang, Y. Sun, A. Trimborn, M. Northway, P.J. Ziemann, M.R. Canagaratna, T.B. Onasch, R. Alfarra, A.S.H. Prevot, J. Dommen, J. Duplissy, A. Metzger, U. Baltensperger, J.L. Jimenez, O/C and OM/OC ratios of primary, secondary, and ambient organic aerosols with high resolution time-of-flight aerosol mass spectrometry, Environ. Sci. Technol. 42 (2008) 4478–4485.
[7] I.M. Ulbrich, M.R. Canagaratna, Q. Zhang, D.R. Worsnop, J.L. Jimenez, Interpretation of organic components from positive matrix factorization of aerosol mass spectrometric data, Atmos. Chem. Phys. 9 (2009) 2891–2918.

[8] J.T. Jayne, D.C. Leard, X. Zhang, P. Davidovits, K.A. Smith, C.E. Kolb, D.R. Worsnop, Development of an aerosol mass spectrometer for size and composition analysis of submicron particles, Aerosol Sci. Technol. 33 (2000) 49–70.
[9] P.F. DeCarlo, E.J. Dunlea, J.R. Kimmel, A.C. Aiken, D. Sueper, J. Crounse, P.O. Wennberg, L. Emmons, Y. Shinozuka, A. Clarke, J. Zhou, J. Tomlinson, D. Collins, D. Knapp, A. Weinheimer, T. Campos, J.L. Jimenez, Fast airborne aerosol size and chemistry measurements above Mexico City and Central Mexico during the MILAGRO campaign, Atmos. Chem. Phys. 8 (2008) 4027–4048.
[10] E. Nemitz, M.A. Sutton, Gas-particle interactions above a Dutch heathland: III. Modelling the influence of the NH3-HNO3-NH4NO3 equilibrium on size-segregated particle fluxes, Atmos. Chem. Phys. 4 (2004) 1025–1045.
[11] G. Buzorius, Ü. Rannik, J.M. Mäkelä, T. Vesala, M. Kulmala, Vertical aerosol particle fluxes measured by eddy covariance technique using condensational particle counter, J. Aerosol Sci. 29 (1998) 157–171.
[12] E. Nemitz, M.A. Sutton, G.P. Wyers, R.P. Otjes, M.G. Mennen, E.M. van Putten, M.W. Gallagher, Gas-particle interactions above a Dutch heathland: II. Concentrations and surface exchange fluxes of atmospheric particles, Atmos. Chem. Phys. 4 (2004) 1007–1024.
[13] R.M. Thomas, I. Trebs, R. Otjes, P.A.C. Jongejan, H. ten Brink, G. Phillips, M. Kortner, F.X. Meixner, E. Nemitz, An automated analyzer to measure surface-atmosphere exchange fluxes of water soluble inorganic aerosol compounds and reactive trace gases, Environ. Sci. Technol. 43 (2009) 1412–1418.
[14] D.D. Baldocchi, B.B. Hicks, T.P. Meyers, Measuring biosphere-atmosphere exchanges of biologically related gases with micrometeorological methods, Ecology 69 (1988) 1331–1340.
[15] E. Nemitz, J.L. Jimenez, J.A. Huffman, I.M. Ulbrich, M.R. Canagaratna, D.R. Worsnop, A.B. Guenther, An eddy-covariance system for the measurement of surface/atmosphere exchange fluxes of submicron aerosol chemical species—first application above an urban area, Aerosol Sci. Technol. 42 (2008) 636–657.
[16] J. Freudenthal, L.G. Gramberg, Pulse-counting techniques in organic mass spectrometry, Anal. Chem. 49 (1977) 2205–2208.
[17] J.D. Ingle, S.R. Crouch, Critical comparison of photon counting and direct current measurement techniques for quantitative spectrometric methods, Anal. Chem. 44 (1972) 785–794.
[18] M. Gonin, K. Fuhrer, A. Schultz, A new concept to increase dynamic range using multi-anode detectors, in: Proceedings of the 48th ASMS Conference on Mass Spectrometry and Allied Topics, Long Beach, CA, June, 2000, TOF Analyzers—11:15.
[19] F. Esposito, N. Spinelli, R. Velotta, Dead time correction of time distribution measurements, Rev. Sci. Instrum. 62 (1991) 2822–2827.
[20] T. Stephan, J. Zehnpfenning, A. Benninghoven, Correction of dead time effects in time-of-flight mass spectrometry, J. Vac. Sci. Technol. A 12 (1994) 405–410.
[21] I.V. Chernushevich, A.V. Loboda, B.A. Thomson, An introduction to quadrupole-time-of-flight mass spectrometry, J. Mass Spectrom. 36 (2001) 849–865.
[22] Y. Ishino, H. Taniguchi, Dead time loss correction of mass errors occurring in high-throughput proteomics based on electrospray ionization time-of-flight tandem mass spectrometry, Rapid Commun. Mass Spectrom. 24 (2010) 1490–1495.
[23] J.R. Kimmel, P.F. DeCarlo, D.R. Worsnop, J.L. Jimenez, Quantitative time-of-flight mass spectrometry of aerosols using a digitally thresholded analog-to-digital converter, Instrumentation—TOFMS—179, in: Proceedings of the 54th ASMS Conference on Mass Spectrometry and Allied Topics, Seattle, WA, May 27–June 2, 2006.
[24] P. Liu, P.J. Ziemann, D. Kittelson, P.H. McMurry, Generating particle beams of controlled dimensions and divergence 2. experimental evaluation of particle motion in aerodynamic lenses and nozzle expansions, Aerosol Sci. Technol. 22 (1995) 314–324.
[25] D. Salcedo, T.B. Onasch, A.C. Aiken, L.R. Williams, B. de Foy, M.J. Cubison, D.R. Worsnop, L.T. Molina, J.L. Jimenez, Determination of particulate lead during MILAGRO/MCMA-2006 using aerosol Mass spectrometry, MILAGRO/MCMA-2006 observations, Atmos. Chem. Phys. 10 (2010) 5371–5389.
[26] G.R. McMeeking, S.M. Kreidenweiss, S. Baker, C.M. Carrico, J.C. Chow, J.L. Collett, W.M. Hao, A.S. Holden, T.W. Kirchstetter, W.C. Malm, H. Moosmuller, A.P. Sullivan, C.E. Wold, Emissions of trace gases and aerosols during the open combustion of biomass in the laboratory, J. Geophys. Res. 114 (2009) D19210.
[27] D.J. Jacob, J.H. Crawford, H. Maring, A.D. Clarke, J.E. Dibb, L.K. Emmons, R.A. Ferrare, C.A. Hostetler, P.B. Russell, H.B. Singh, A.M. Thompson, G.E. Shaw, E. McCauley, J.R. Pederson, J.A. Fisher, The arctic research of the composition of the troposphere from aircraft and satellites (ARCTAS) mission: design, execution, and first results, Atmos. Chem. Phys. 10 (2010) 5191–5212.
[28] A.H. Goldstein, N.E. Hultman, J.M. Fracheboud, M.R. Bauer, J.A. Panek, M. Xu, Y. Qi, A.B. Guenther, W. Baugh, Effects of climate variability on the carbon dioxide, water, and sensible heat fluxes above a ponderosa pine plantation in the Sierra Nevada (CA), Agric. Forest Meteorol. 101 (2000) 113–129.
[29] D.K. Farmer, J.R. Kimmel, G. Phillips, K.S. Docherty, D.R. Worsnop, D. Sueper, E. Nemitz, J.L. Jimenez, Eddy-covariance measurements with high-resolution time-of-flight aerosol mass spectrometry: a new approach to chemically resolved aerosol fluxes, Atmos. Meas. Technol. Discuss. 3 (2010) 5867–5905.